CMS Physics Analysis Summary

Contact: cms-pag-conveners-exotica@cern.ch 2011/06/10

Search for Black Holes in pp collisions at $\sqrt{s} = 7$ TeV

The CMS Collaboration

Abstract

An update on a search for microscopic black hole production in pp collisions at a center-of-mass energy of 7 TeV by the CMS experiment at the LHC is presented using a 2011 data sample corresponding to an integrated luminosity of 190 pb^{-1}. This corresponds to a six-fold increase in statistics compared to the original search based on 2010 data. Events with large total transverse energy have been analyzed for the presence of multiple energetic jets, leptons, and photons, typical of a signal from an evaporating black hole. A good agreement with the expected standard model backgrounds, dominated by QCD multijet production, has been observed for various multiplicities of the final state. Stringent model-independent limits on new physics production in high-multiplicity energetic final states have been set, along with model-specific limits on semi-classical black hole masses in the 4-5 TeV range for a variety of model parameters. This update extends substantially the sensitivity of the 2010 analysis.

One of the exciting predictions of theoretical models with extra spatial dimensions and low-scale quantum gravity is the possibility of copious production of black holes in particle collisions at the LHC [1, 2]. Such models are candidates for a theory beyond the standard model (SM). They are mainly motivated by the puzzling large difference between the electroweak scale ($\sim$ 1 TeV) and the Planck scale ($\sim 10^{16}$ TeV), and attempt to solve this hierarchy problem. In this analysis we focus on black hole production in a model with large, flat, extra spatial dimensions (ADD model) [3, 4].

In this PAS, we present an extension of the published first search for black holes at a hadron collider [5] carried out by the CMS Collaboration in 2010. We present an update of this search based on a six-fold increase in statistics already collected in the 2011 LHC data-taking period. This search is based exclusively on the 2011 data sample corresponding to an integrated luminosity of 190 ± 8 pb^{-1}.[1] The details of the CMS detector [7], analysis method, underlying theory, as well as the detailed description of models we probed in this search can be found in the original publication [5].

As in the 2010 analysis, we used data collected with a suite of H_T triggers, where H_T is defined as a scalar sum of the transverse energies (E_T) of the jets above a preprogrammed threshold[2]. There have been certain changes introduced in the trigger logic both at Level 1 (L1) and at the High-Level Trigger (HLT) since 2010. Namely, we now use jets corrected for the calorimeter response to calculate the H_T variable at the HLT (uncorrected jets are still used at L1), and the minimum H_T thresholds, as well as the minimum jet E_T requirement for a jet to be counted toward H_T have been increased to alleviate effects of the pile-up and match the increased instantaneous luminosity of the machine. This minimum jet E_T threshold was 10 GeV at L1, and 40 GeV at the HLT. The minimum H_T threshold at the HLT was varied between 350 and 550 GeV, depending on the running period. Only jets found at central rapidities $|\eta| < 3.0$ are used toward the H_T calculations at L1, and at the HLT for the later portion of the data taking period. The trigger has been shown to be fully efficient for the minimum offline H_T requirement of 700 GeV, and hence it is fully efficient for the offline cuts used in the analysis.

Offline, jets are reconstructed using energy deposits in the HCAL and ECAL, which are clustered using an infrared-safe anti-k_T algorithm with the distance parameter of 0.5 [8]. The jet energy resolution is $\Delta E/E \approx 100\,\%/\sqrt{E} \oplus 5\,\%$. Jets are required to pass standard quality requirements to remove the ones consistent with calorimeter noise [9]. Jet energies are corrected for the non-uniformity and non-linearity of the calorimeter response derived using Monte Carlo (MC) samples and collision data [10]. We require jets to have transverse energy above 20 GeV before jet energy scale corrections and to have $|\eta| < 2.6$. Missing transverse energy ($\not\!\!E_T$) is reconstructed as a negative vector sum of transverse energies in the individual calorimeter towers and is further corrected for the jet energy scale and muons in the event, which leave little energy deposit in the calorimeter [11].

Electrons and photons are reconstructed as isolated energy deposits in the ECAL with a shape consistent with that expected for the electromagnetic showers. The ECAL energy resolution is better than 0.5 % above 100 GeV. Photons are required to have no matching hits in the inner pixel detector layers, while electrons were required to have a matching track. Electrons and photons are required to have $E_T > 20$ GeV and to be reconstructed in the fully instrumented barrel ($|\eta| < 1.44$) or end-cap ($1.56 < |\eta| < 2.4$) region.

[1] We assume a 4% uncertainty on the integrated luminosity, as was the case in 2010 running [6]. The determination of the 2011 luminosity uncertainty is under way. While we expect it to be close to that in 2010, we checked that changing this uncertainty from 4% to 10% does not affect the limits within the quoted precision.

[2] Energetic electrons and photons are also reconstructed as jets at the trigger level.

Muons are required to have a match between the stand-alone muon spectrometer and the central tracker, to be within $|\eta| < 2.1$, be consistent with the interaction vertex to suppress backgrounds from cosmic muons, and have $p_T > 20$ GeV. Matching the muons to the tracks measured in the silicon tracker results in a transverse momentum resolution between 1% and 5% for p_T values up to 1 TeV. The minimum separation between any two objects (jet, lepton, or photon) is required to be $\Delta R = \sqrt{\Delta\phi^2 + \Delta\eta^2} < 0.3$.

Simulated samples of black hole signal events are generated using a parton-level BlackMax [12] generator (v2.01), followed by the parton showering simulation with PYTHIA [13] (v6.420), and a fast parametric simulation of the CMS detector [14, 15]. The parameters used in simulation are listed in Table 1 for a few characteristic model points. The MSTW2008lo68 [16] parton distribution functions (PDF) were used. In addition, we compared the results with CHARYBDIS [17, 18] MC generator (CHARYBDIS 2, v1.0.3). The BlackMax and CHARYBDIS use different values of the total cross section, since there is an additional factor (which depends on the number of extra dimensions n) in front of the pure geometrical cross section used in BlackMax. The CHARYBDIS cross sections are a factor of 1.36, 1.59, and 1.78 smaller than those from BlackMax for $n = 2$, 4, and 6, respectively. These scale factors can be used to interpret our results in the CHARYBDIS framework. In addition, we used CHARYBDIS to simulate black hole evaporation resulting in a stable remnant with the mass M_D (this model is not implemented in BlackMax).

We employ a selection based on total transverse energy to separate black hole events from the backgrounds. We define the S_T variable as a scalar sum of the E_T of individual jets, electrons, photons, and muons passing the above selections. Only objects with $E_T > 50$ GeV are counted toward the S_T. The choice of this rather high minimum transverse energy requirement is driven by the fact that it suppresses most of the copious SM processes and is insensitive to the jets from pile-up, while fully efficient for black hole decays. We further add $\not\!\!E_T$ in the event to the S_T, if the $\not\!\!E_T$ value exceeds 50 GeV. Generalization of the S_T definition to include $\not\!\!E_T$ is important for testing black hole models with significant amount of missing energy, e.g. the models with a stable non-interacting remnant. We checked that in case jets are mismeasured and as a result a non-genuine $\not\!\!E_T$ is generated in the event, the effect of the "double-counting" of this mismeasurement in both jet and $\not\!\!E_T$ contributions to the S_T is negligible.

Main background to black hole production arises from multijet and direct photon production, which dominates the event rates at large S_T. Smaller backgrounds come from W/Z+jets production, and $t\bar{t}$. These backgrounds are negligible at large values of S_T and contribute less than 1% to the total background after the final selection. We estimate their contribution from MC simulation, using MADGRAPH [19] leading-order parton-level event generator with CTEQ6L PDF set [20] followed by PYTHIA [13] parton showering and full CMS detector simulation via GEANT4 [21]. For the dominant QCD background, however, we estimate backgrounds from data using the S_T multiplicity invariance technique of Ref. [5]. This technique is based on the independence of the shape of the S_T spectrum on the number of the final state objects N; an empirical observation extensively checked and proved correct by using various MC samples and low-multiplicity data. This invariance allows us to predict the shape of the S_T spectrum for any number of objects using the dijet data, which has been extensively studied for presence of new physics in dedicated analyses [22–24].

We fit the S_T distributions in data with $N = 2$ and $N = 3$ between 700 and 1500 GeV (where no evidence for new physics has been observed in a dedicated analysis [22]) with the ansatz function $\frac{P_0(1+x)^{P_1}}{x^{P_2+P_3\log(x)}}$, which is shown with the solid line in Fig. 1. To check the systematic uncertainty of the fit, we use two additional ansatz functions, $\frac{P_0}{(P_1+P_2x+x^2)^{P_3}}$ and $\frac{P_0}{(P_1+x)^{P_2}}$, which are shown as

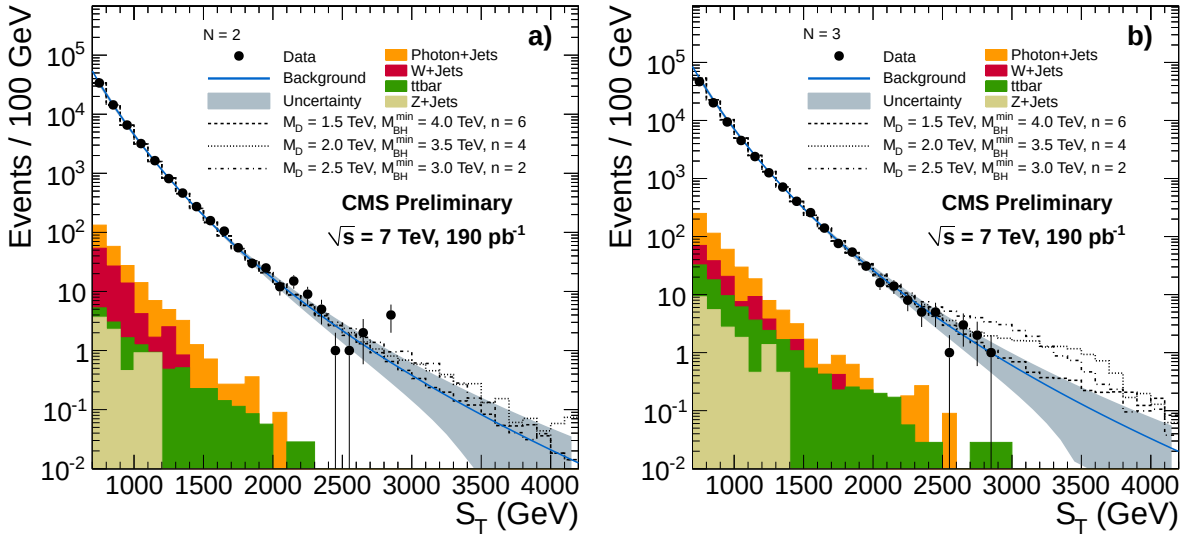

Figure 1: Total transverse energy, S_T, for events with a) $N = 2$, and b) $N = 3$ objects in the final state. Data are depicted as solid circles with error bars; shaded band is the data-driven background prediction (solid line) with its uncertainty. Non-QCD backgrounds are shown as colored histograms. Also shown is black hole signal for three different parameter sets, demonstrating small signal contamination.

the upper and lower boundaries of the shaded curve in Fig. 1. The default choice of the ansatz function is based on the best fit χ^2 to the S_T distribution for $N = 2$. Additional systematic uncertainty arises from a slight difference between the best fit shapes for $N = 2$ and $N = 3$. Nevertheless, the fits for these two exclusive multiplicities are very consistent and agree with each other within the uncertainties, demonstrating independence of the S_T shape on the final state multiplicity.

We then look at the inclusive samples with high multiplicity using the background shape from the low multiplicity distributions, as shown in Fig. 2, normalized to the inclusive data in the range of 1300 – 1500 GeV, where no signal contribution is expected. The data agree well with the background shapes from the low-multiplicity samples and do not exhibit any evidence for new physics. An event display of one of the black-hole candidate event ($N = 10$, $S_T = 1.1$ TeV) is shown in Fig. 3. The relatively high minimum requirement on jet transverse energy of 50 GeV to be counted toward N and S_T essentially eliminate jets from pile-up, which is evident from the zoom on the vertex region in this figure, which demonstrates that all 10 jets originate from the common, primary vertex.

Since no excess is observed above the predicted background, we proceed with setting limits on black hole production. We assign systematic uncertainty on the background estimate varying from 4% to 138% in the S_T range used in this search. This uncertainty comes from the normalization uncertainty (2 – 6%) added in quadrature to the uncertainties from using various fit ansatz functions and the difference between the shapes obtained from the $N = 2$ and $N = 3$ samples. The integrated luminosity is measured *in situ* using forward calorimeters with 4% uncertainty [6]. Signal uncertainty is dominated by the jet energy scale uncertainty of $\approx 5\%$ [10] which translates into 5% uncertainty on the signal. An additional 2% uncertainty on the signal acceptance comes from the variation of PDFs within the CTEQ6 error set [20]. Note that particle identification efficiency does not affect the signal distribution, since if an electron does not pass the identification requirements it is either classified as a photon, or as a jet; a photon failing the selection will become a jet; and a rejected muon will contribute to $\not\!\!E_T$. Thus, the total S_T in the

Table 1: Monte Carlo signal points for some of the model parameters probed, corresponding leading order cross sections, and optimal selections on the minimum decay multiplicity ($N \geq N^{\min}$) and minimum S_T, as well as signal acceptance, expected number of signal events, number of observed events in data, expected background, and observed and expected limit on the signal at 95% confidence level.

M_D (TeV)	M_{BH} (TeV)	n	σ (pb)	$N^{\min}$	$S_T^{\min}$ (TeV)	A (%)	N^{sig}	N^{data}	N^{bkg}	σ^{95} (pb)	$\langle\sigma^{95}\rangle$ (pb)
1.5	2.5	6	117.90	3	1.5	90.6	20300	1507	1442 ± 144	1.67	0.51
1.5	3.0	6	25.94	3	1.8	91.3	4510	357	356 ± 73	0.29	0.34
1.5	3.5	6	4.97	4	2.1	88.3	836	50	59.8 ± 20.1	0.14	0.17
1.5	4.0	6	0.77	5	2.4	84.4	123	6	8.95 ± 4.40	0.04	0.05
1.5	4.5	6	0.09	5	2.8	83.8	14.5	1	2.35 ± 1.73	0.02	0.03
1.5	5.0	6	0.01	6	3.3	73.7	1.00	0	$0.19^{+0.22}_{-0.19}$	0.02	0.02
2.0	2.5	4	28.88	3	1.7	81.4	4480	541	556 ± 93	0.33	0.38
2.0	3.0	4	6.45	3	2.0	83.2	1020	137	153 ± 44	0.29	0.28
2.0	3.5	4	1.26	3	2.4	80.0	191	26	33.7 ± 16.5	0.11	0.12
2.0	4.0	4	0.20	4	2.7	77.3	29.3	4	7.08 ± 4.75	0.04	0.05
2.0	4.5	4	0.02	5	3.1	68.3	3.06	0	0.94 ± 0.90	0.02	0.02
2.0	5.0	4	0.00	6	3.6	54.7	0.19	0	$0.09^{+0.12}_{-0.09}$	0.03	0.02
2.5	3.0	2	0.97	3	2.3	67.0	123	36	48.3 ± 21.0	0.16	0.16
2.5	3.5	2	0.19	3	2.7	64.6	23.6	7	12.2 ± 8.2	0.06	0.06
2.5	4.0	2	0.03	4	3.1	55.5	3.32	0	2.06 ± 1.97	0.03	0.03
2.5	4.5	2	0.00	5	3.4	47.2	0.35	0	$0.40^{+0.49}_{-0.40}$	0.03	0.02
2.5	5.0	2	0.00	6	3.9	31.2	0.02	0	$0.04^{+0.07}_{-0.04}$	0.05	0.02

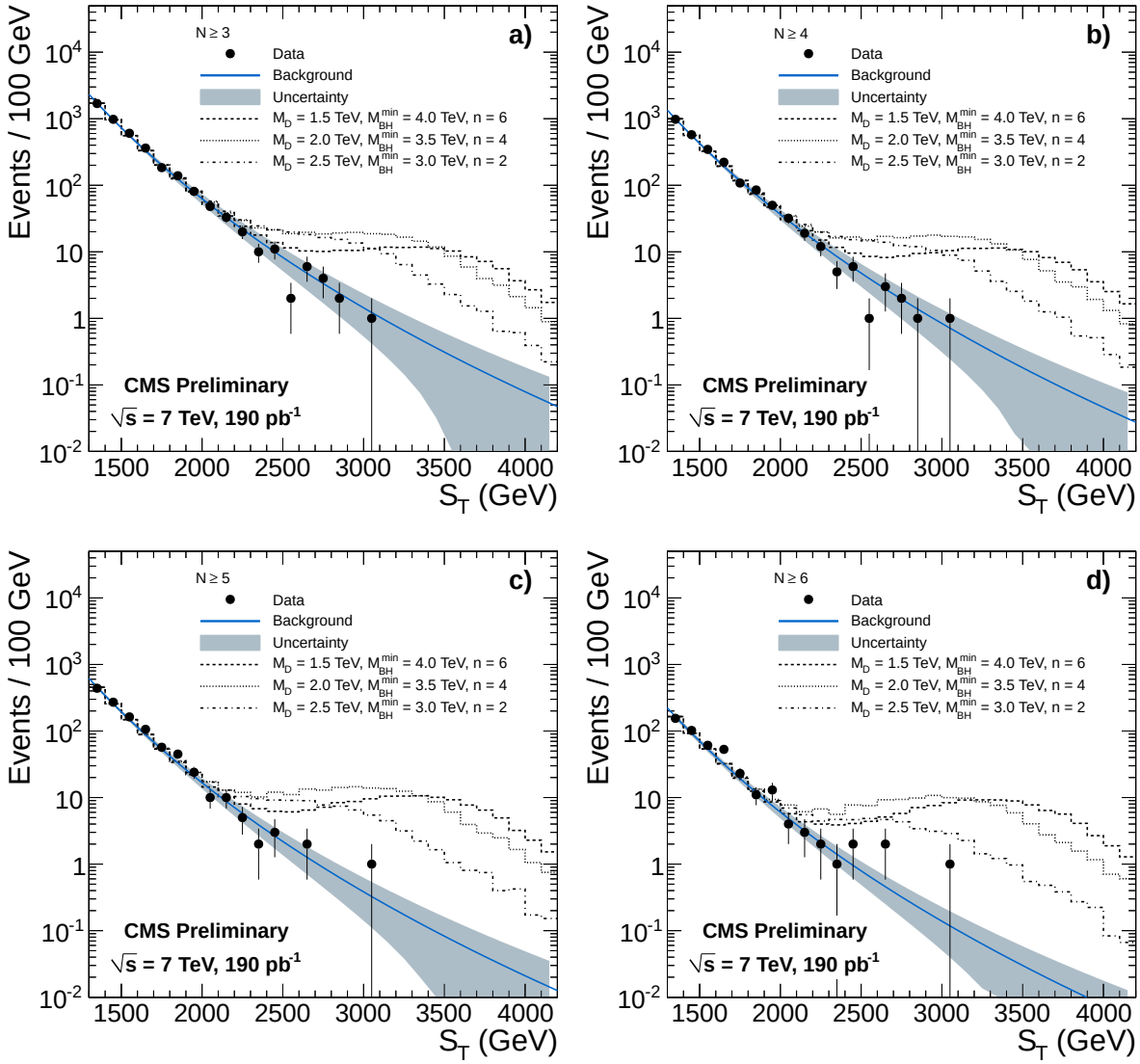

Figure 2: Total transverse energy, S_T, for events with: a) $N \geq 3$, b) $N \geq 4$, c) $N \geq 5$, and d) $N \geq 6$ objects in the final state. Data are depicted as solid circles with error bars; shaded band is the background prediction (solid line) with its uncertainty. Also shown are black hole signals for three different parameter sets.

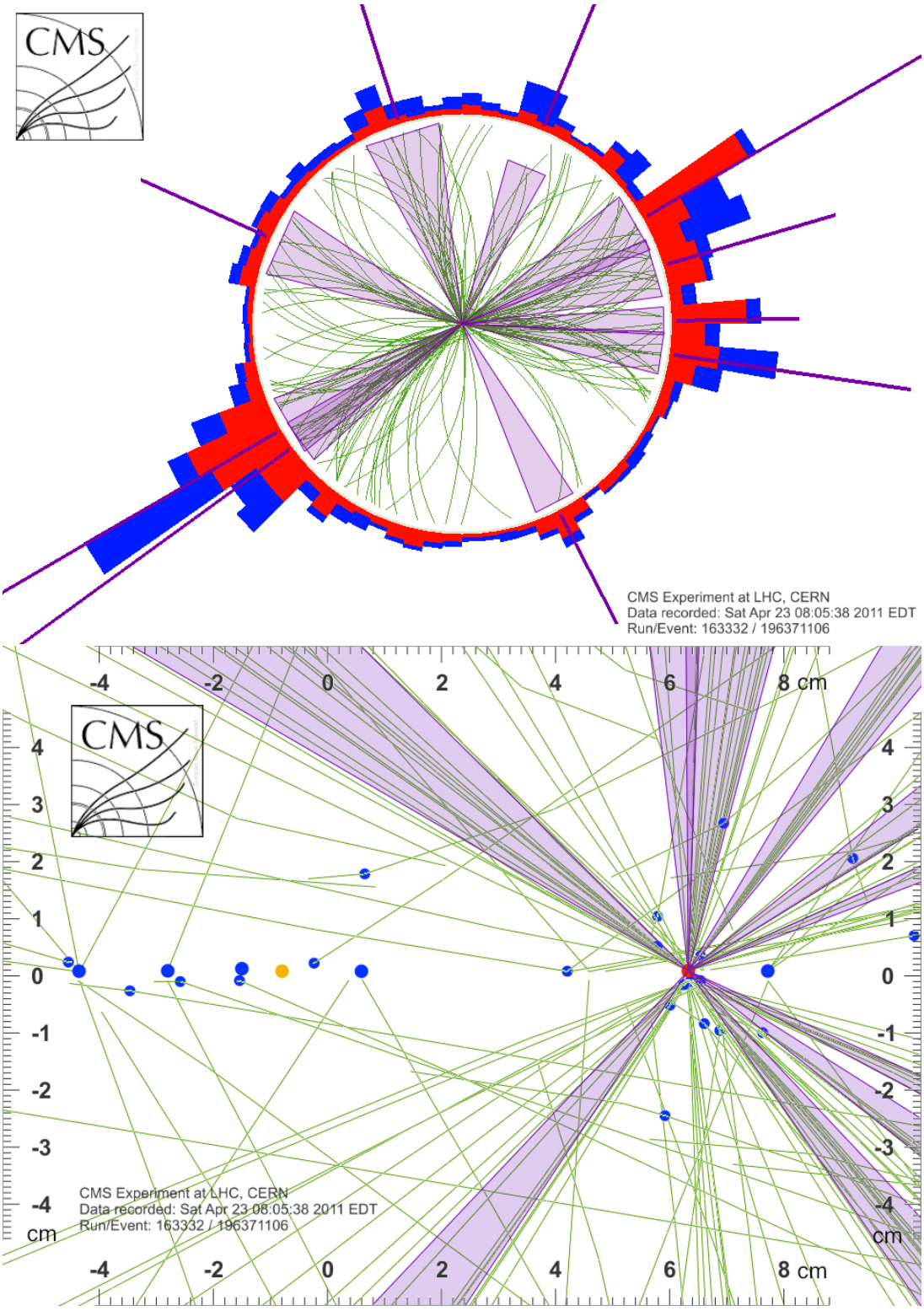

Figure 3: An event display of a $N = 10$ black hole candidate with $S_T = 1.1$ TeV (Run 163332, Event 196371106). Top: the transverse view of the event with 10 objects (jets) highlighted with magenta cones. Bottom: the zoom on the vertex region in the view parallel to the beam-line. All the jets clearly come from the same, primary vertex (red dot), despite a number of pile-up vertices (blue dots). The nominal beam-spot position is shown with an orange dot.

event is virtually not affected.

Given how significant model-dependence of the black hole production cross section and decay patterns are, it is virtually impossible to test all different variations of model parameters offered by modern black hole MC generators in a dedicated search. This study considers over 160 different signal MC samples already, and yet it does not come close to spanning the entire parameter space of the model. Hence, we choose to first present the results of our search in a generic, model-independent way, which would allow to probe additional models essentially using parton-level MC information (possibly augmented with very crude detector simulation). To facilitate that, we produce model-independent limits on the cross section times the acceptance for new physics production in high-S_T inclusive final states for $N \geq 3, 4, 5$, and 6. Figure 4 shows 95% confidence level (CL) limits from a counting experiment for $S_T > S_T^{\min}$ as a function of $S_T^{\min}$, which can be used to test models of new physics that result in these final state, including (but not limited to) even broader variety of black hole models that we covered in this analysis. The 95% CL limits from 2010 data [5] are also shown in Fig. 4. The present model-independent limits are roughly 15 fb at high values of S_T, which is six times the limits reported in the previous publication [5] – in good agreement with expectations given six-fold increase in integrated luminosity. Given higher statistics of the 2011 sample, we are also able to extend these limits to the $N \geq 6$ case, which was not possible before.

For specific subset of the black hole models we probe [5], we also set dedicated limits on black hole production with the optimized S_T and N selections using counting experiments. We optimized the signal (S) significance in the presence of background (B), $S/\sqrt{S+B}$, for each set. The optimum choices of parameters are listed in Table 1, as well as the predicted number of background events, expected number of signal events, and the observed number of events in data. We set limits using a Bayesian method with a flat signal prior and a log-normal prior for integration over the nuisance parameters. These limits at the 95% confidence level (CL) are shown in Fig. 5.

Translating the cross section limits into the expectations of the ADD model, we can exclude the production of black holes with a minimum mass varying from 3.7 to 4.8 TeV for values of the multidimensional Planck scale up to 3.5 TeV at 95% CL. These limits, shown in Fig. 6, do not exhibit a significant dependence on the details of the production and evaporation model and are the first limits of a dedicated search for black hole production at hadron colliders.

To conclude, we presented an update of an earlier published first dedicated search for black holes at a hadron collider [5] and set stringent model-independent limits on the production of energetic multi-particle final states, which can be used to constrain a large variety of models of new physics. In addition we set model-specific stringent limits on the minimum black hole mass in the $4-5$ TeV range for a large variety of model parameters.

References

[1] S. Dimopoulos and G. Landsberg, "Black Holes at the LHC", *Phys. Rev. Lett.* **87** (2001) 161602, arXiv:hep-ph/0106295. doi:10.1103/PhysRevLett.87.161602.

[2] S. Giddings and S. Thomas, "High-energy colliders as black hole factories: The end of short distance physics", *Phys. Rev. D* **65** (2002) 056010, arXiv:hep-ph/0106219. doi:10.1103/PhysRevD.65.056010.

[3] N. Arkani-Hamed, S. Dimopoulos, and G. Dvali, "The Hierarchy problem and new dimensions at a millimeter", *Phys. Lett. B* **429** (1998) 263–267.

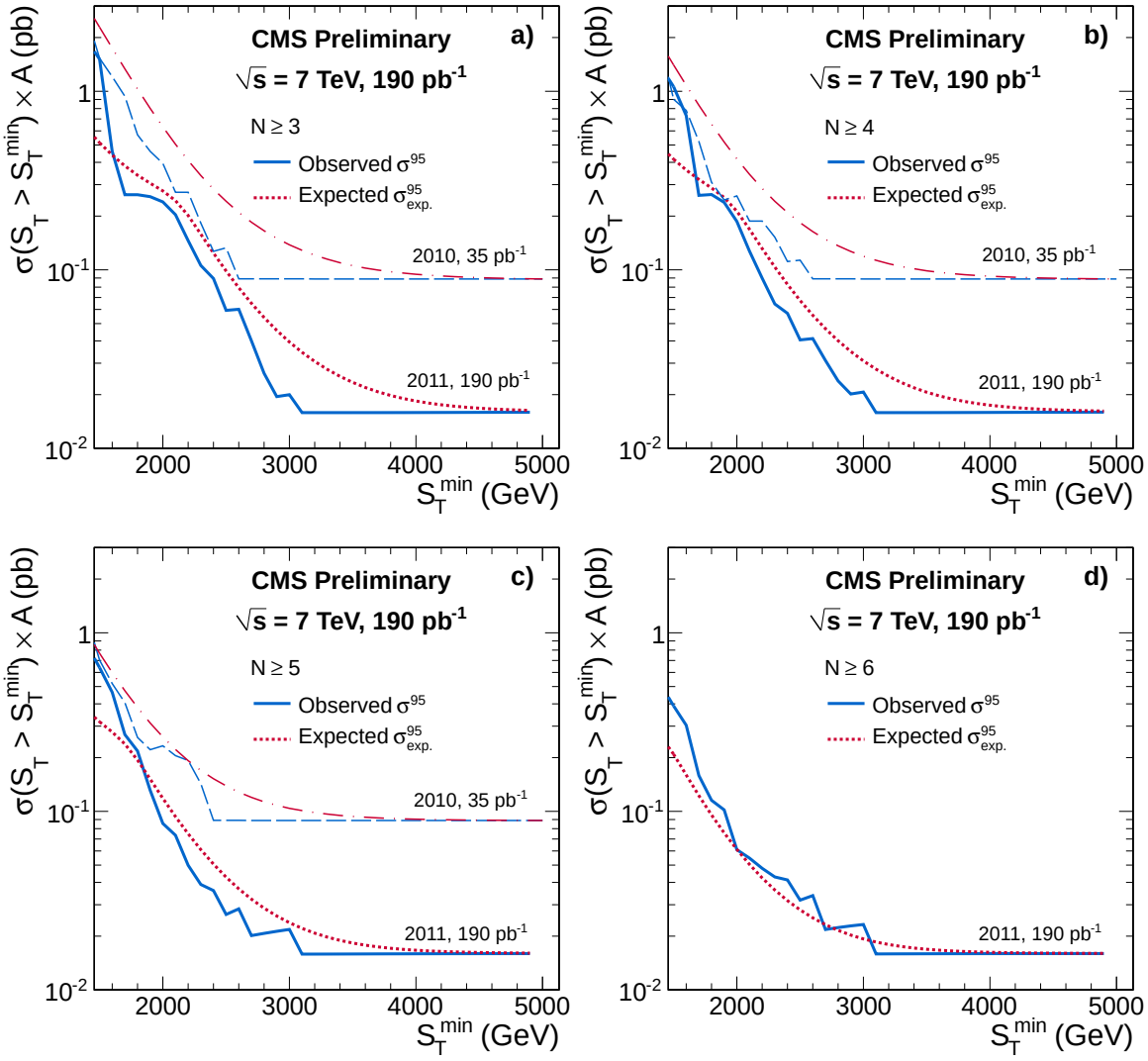

Figure 4: Model-independent 95% confidence level upper cross section limits for counting experiments with $S_T > S_T^{\min}$ as a function of $S_T^{\min}$ for a) $N \geq 3$, b) $N \geq 4$, c) $N \geq 5$, and d) $N \geq 6$. The blue solid (red dotted) lines correspond to an observed (expected) limit for nominal signal acceptance uncertainty of 5%, compared to observed (expected) limits obtained on 2010 CMS data and shown as blue dashed (red dash-dotted) line.

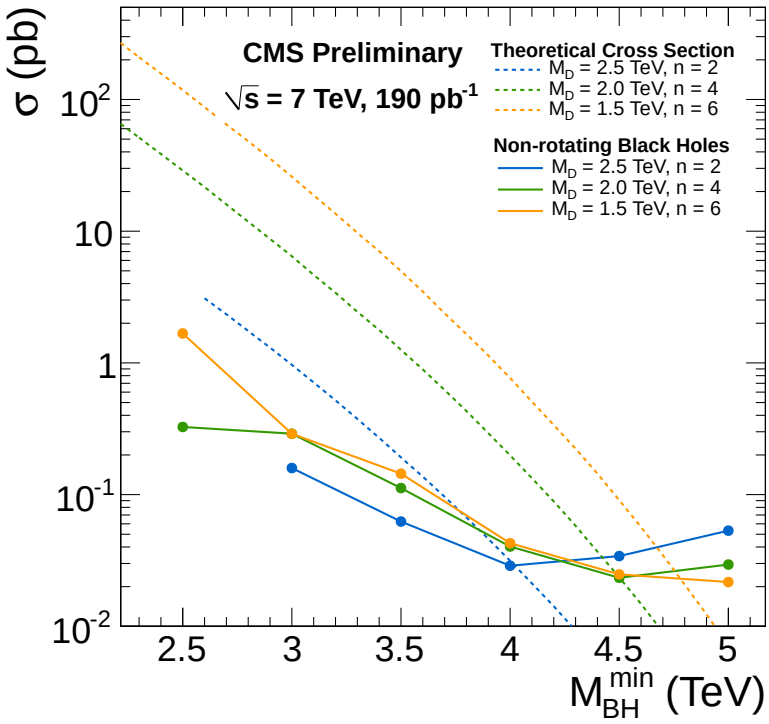

Figure 5: Cross section limits at 95% confidence level from the counting experiments optimized for various black hole parameter sets compared with signal production cross section. Colored solid lines show experimental cross section limits, while dotted lines represent corresponding signal cross sections. The corresponding expected limits are 3.9, 4.5, and 4.8 TeV.

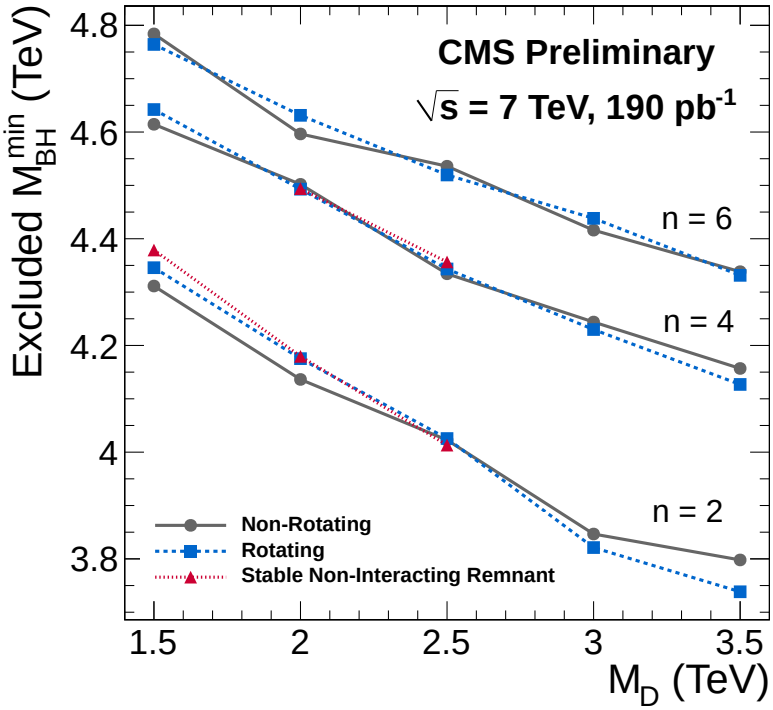

Figure 6: Limits on the black hole model parameters for several benchmark scenarios. The areas below each curve are excluded by this search.

doi:10.1016/S0370-2693(98)00466-3.

[4] N. Arkani-Hamed, S. Dimopoulos, and G. Dvali, "Phenomenology, astrophysics and cosmology of theories with submillimeter dimensions and TeV scale quantum gravity", *Phys. Rev. D* **59** (1999) 086004. doi:10.1103/PhysRevD.59.086004.

[5] CMS Collaboration, "Search for Microscopic Black Hole Signatures at the Large Hadron Collider", *Phys. Lett.* **B697** (2011) 434–453, arXiv:1012.3375. doi:10.1016/j.physletb.2011.02.032.

[6] CMS Collaboration, "Measurement of CMS Luminosity", (2011). CMS-DP-2011-002. Document in preparation.

[7] CMS Collaboration, "The CMS experiment at the CERN LHC", *JINST* **3** (2008) S08004. doi:10.1088/1748-0221/3/08/S08004.

[8] M. Cacciari, G. Salam, and G. Soyez, "The anti-k_T jet clustering algorithm", *Journal of High Energy Physics* **2008** (2008), no. 04, 063. doi:10.1088/1126-6708/2008/04/063.

[9] CMS Collaboration, "Jet Performance in pp Collisions at 7 TeV", CMS PAS JME-10-003.

[10] CMS Collaboration, "Jet Energy Corrections determination at $\sqrt{s} = 7$ TeV", CMS PAS JME-10-010.

[11] CMS Collaboration, "Missing Transverse Energy Performance in Minimum-Bias and Jet Events from Proton-Proton Collisions at $\sqrt{s} = 7$ TeV", CMS PAS JME-10-004.

[12] D.-C. Dai, G. Starkman, D. Stojkovic et al., "BlackMax: A black-hole event generator with rotation, recoil, split branes, and brane tension", *Phys. Rev. D* **77** (2008), no. 7, 076007. doi:10.1103/PhysRevD.77.076007.

[13] T. Sjöstrand, S. Mrenna, and P. Skands, "PYTHIA 6.4 Physics and Manual", *JHEP* **05** (2006) 026. doi:10.1088/1126-6708/2006/05/026.

[14] D. Orbaker, "Fast Simulation of the CMS Detector", CERN-CMS-CR-2009-074.

[15] S. Abdullin, P. Azzi, F. Beaudette et al., "Fast Simulation of the CMS Detector at the LHC", CERN-CMS-CR-2010-297.

[16] MSTW Collaboration, "Heavy-quark mass dependence in global PDF analyses and 3- and 4-flavour parton distributions", arXiv:1007.2624.

[17] C. M. Harris, P. Richardson, and B. R. Webber, "CHARYBDIS: A black hole event generator", *JHEP* **08** (2003) 033, arXiv:hep-ph/0307305.

[18] J. Frost et al., "Phenomenology of Production and Decay of Spinning Extra- Dimensional Black Holes at Hadron Colliders", *JHEP* **10** (2009) 014, arXiv:0904.0979. doi:10.1088/1126-6708/2009/10/014.

[19] J. Alwall et al., "MadGraph/MadEvent v4: The New Web Generation", *JHEP* **09** (2007) 028. doi:10.1088/1126-6708/2007/09/028.

[20] CTEQ Collaboration, "Implications of CTEQ global analysis for collider observables", *Phys. Rev. D* **78** (2008) 013004.

[21] GEANT 4 Collaboration, "GEANT4 – a simulation toolkit", *Nucl. Instr. and Methods A* **506** (2003) 250–303. doi:10.1016/S0168-9002(03)01368-8.

[22] CMS Collaboration, "Search for Dijet Resonances in 7 TeV pp Collisions at CMS", *Phys. Rev. Lett.* **105** (2010) 211801, arXiv:1010.0203. doi:10.1103/PhysRevLett.105.21180.

[23] CMS Collaboration, "Search for Quark Compositeness with the Dijet Centrality Ratio in pp Collisions at $\sqrt{s} = 7$ TeV", *Phys. Rev. Lett.* **105** (2010) 262001, arXiv:1010.4439. doi:10.1103/PhysRevLett.105.262001.

[24] CMS Collaboration, "Measurement of Dijet Angular Distributions and Search for Quark Compositeness in pp Collisions at 7 TeV", *Phys. Rev. Lett.* **106** (2010) 201804, arXiv:1102.2020. doi:10.1103/PhysRevLett.106.201804.